

Title	Photoanodic Properties of Plasma Sprayed TiO <sub>2</sub> Coatings(Surface Processing)
Author(s)	Ohmori, Akira; Park, Kyeong-Chae; Arata, Yoshiaki et al.
Citation	Transactions of JWRI. 1990, 19(2), p. 271-275
Version Type	VoR
URL	<a href="https://doi.org/10.18910/12265">https://doi.org/10.18910/12265</a>
rights	
Note	

*Osaka University Knowledge Archive : OUKA*

<https://ir.library.osaka-u.ac.jp/>

Osaka University

# Photoanodic Properties of Plasma Sprayed TiO<sub>2</sub> Coatings<sup>†</sup>

Akira OHMORI\*, Kyeung-Chae PARK\*\*, Yoshiaki ARATA\*\*\*,  
Katsunori INOUE\*\*\*\* and Mobuya IWAMOTO\*\*\*\*

## Abstract

*Plasma spraying has been used to prepare n-type polycrystalline TiO<sub>2</sub> coatings on titanium substrate as photoanodes. The photoanodic properties of plasma sprayed TiO<sub>2</sub> coatings depend on the extent of oxygen loss and impurity of TiO<sub>2</sub> particles during plasma spraying. These properties depending on plasma conditions, additives and heat treatment are elucidated in oxygen saturated solution of 0.1 N NaOH.*

*It is shown that the plasma spray atmosphere and plasma auxiliary gas, hydrogen, influence greatly the photoanodic properties of TiO<sub>2</sub> coatings. Moreover, the photoanodic current increases by heat treatment (400°C-90 min) in air and by addition of Y<sub>2</sub>O<sub>3</sub> to TiO<sub>2</sub> coatings.*

*Bandgap (BG) and subbandgap (SBG) photocurrent transients of TiO<sub>2</sub> coatings electrode were explored as a function of the external applied bias and light wavelength. These photocurrent transients disappear at high anodic potentials and increase at high cathodic potentials.*

*Kinetic response of an anodic photocurrent which shows spike immediately and again increases with time after the light is turned on for plasma sprayed TiO<sub>2</sub> coatings, has been discussed with impurity center.*

**KEY WORDS:** (Plasma Spraying) (Additive) (Heat Treatment) (Photoanodic Property) (Impurity Center)

## 1. Introduction

The water decomposition by an electrochemical cell with n-TiO<sub>2</sub> electrode was first demonstrated by Fujishima and Honda<sup>1)</sup>. The process occurs when the TiO<sub>2</sub> electrode is illuminated by light of energy larger than the band gap ( $E_g=3.0$  eV).

In such a case, because of the difference in the work function between TiO<sub>2</sub> and the electrolyte, the Schottky barrier is formed at the semiconductor-electrolyte interface. Electron-hole pair created by the incident photons are separated by the electric field of the barrier; the electrons move away from the surface into the bulk of TiO<sub>2</sub>, whereas the holes accumulate at the TiO<sub>2</sub>-electrolyte interface. At the interface, the holes discharge with hydroxyl ions evolving oxygen gas; the electrons move through the external circuit and discharge with protons at the counterelectrode evolving hydrogen gas<sup>2)</sup>.

Polycrystalline n-TiO<sub>2</sub> has been widely studied as a semiconducting electrode in photoelectrochemical cells. Several techniques for the preparation of the photoanodes are found in the literature, namely, thermal oxidation<sup>3)</sup>, anodic oxidation<sup>4)</sup>, chemical vapor deposition<sup>5)</sup>, sputtering<sup>6)</sup>, sintering<sup>7)</sup> and sprayed coatings<sup>8)</sup>.

Plasma spraying is a well known technique in various industrial fields to obtain the reliable coatings of ceramics and would be practically well suited for large scale production. When TiO<sub>2</sub> (rutile) powders are plasma-sprayed, the TiO<sub>2</sub> coatings become a n-semiconductor whose properties depend on the extent of oxygen loss of TiO<sub>2</sub> particles during plasma spraying. The photoanodic properties of TiO<sub>2</sub> coatings depend greatly on plasma conditions and additives.

In this study, the photoanodic properties of plasma sprayed TiO<sub>2</sub> coatings were studied. And, effects of plasma spray atmosphere, existence of H<sub>2</sub> in plasma gas, additives and heat treatment on photoanodic properties of TiO<sub>2</sub> electrodes were discussed. The plasma spraying was used to prepare n-polycrystalline TiO<sub>2</sub> coatings on titanium-substrate. The photoanodic properties of the plasma sprayed TiO<sub>2</sub> electrodes were measured in oxygen-saturated solutions of 0.1 N NaOH.

## 2. Materials and Experimental Procedure

Materials used in this investigations were commercially available TiO<sub>2</sub> powders (M-102: METCO Ltd and PC-T: Nihon Abrasion Ltd) and titanium plate (25 mm×15 mm×3 mm) as substrate. The

<sup>†</sup> Received on November 5, 1990

\* Associate Professor

\*\* Graduate Student

\*\*\* Emeritus Professor

\*\*\*\* Professor

Transactions of JWRI is published by Welding Research Institute of Osaka University, Ibaraki, Osaka 567, Japan

crystal structure of these powders is rutile. Plasma sprayed  $\text{TiO}_2$  coatings were prepared as photoanodes. **Table 1** shows chemical compositions of these powders.

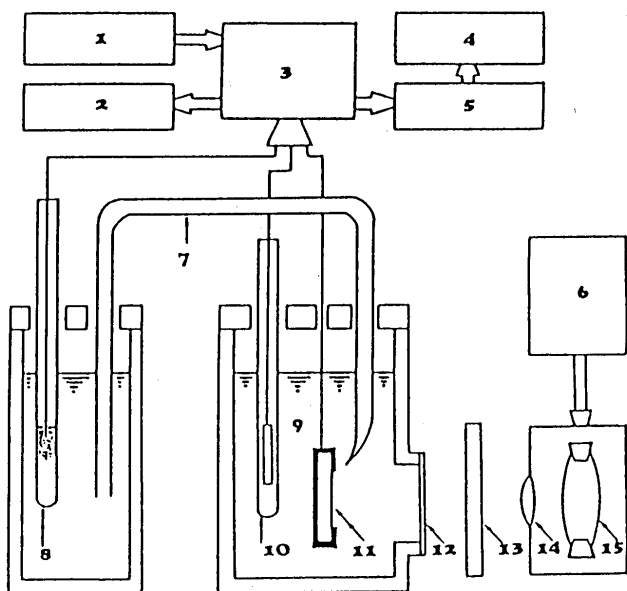
Plasma spraying was performed with a plasma spray system—METCO 7 M. Spraying environment was ambient air, and plasma working gas were Ar (100 l/min) and Ar (100 l/min)+ $\text{H}_2$  (10 l/min). Plasma power was 38 kW and spraying distances were 100 mm. and as additives added to M102- $\text{TiO}_2$  powders, various metal and oxide powders (purity; 99.99wt%) were used.

After plasma spraying, the coatings were heat-treated in the electrical furnace under ambient air and they were cooled slowly in furnace from heat treated temperature to room temperature.

In order to perform the measurement of photoanodic properties, ohmic contacts were established by directly attaching a copper wire to the conducting substrate-Ti plate. All the nonphotoactive parts of the photoelectrode were afterwards covered with silicone rubber to

**Table 1** Chemical compositions of plasma spray  $\text{TiO}_2$  powders (wt %).

	$\text{TiO}_2$	$\text{Al}_2\text{O}_3$	$\text{SiO}_2$	$\text{Fe}_2\text{O}_3$	$\text{CaO}$	$\text{HgO}$	$\text{Na}_2\text{O}$
PC-T	99.2	0.20	0.12	0.42	0.03	0.06	0.02
H-102	98.6	1.03	0.08	0.07	0.13	0.05	0.04



- |                               |                             |
|-------------------------------|-----------------------------|
| 1 Function generator          | 9 0.1N NaOH-aq.             |
| 2 X-Y recorder                | 10 Counter Pt electrode     |
| 3 Potentiostat                | 11 $\text{TiO}_2$ electrode |
| 4 Personal computer           | 12 Quartz window            |
| 5 Multimeter                  | 13 Optical filter           |
| 6 Power supply                | 14 Quartz lens              |
| 7 Salt bridge                 | 15 Xe lamp                  |
| 8 Saturated calomel electrode |                             |

**Fig. 1** Photoelectrolysis apparatus with side view of cell.

avoid photoresponse, leaving an active area of  $1 \text{ cm}^2$ .

The measurements of photoanodic properties were performed using a three electrode cell equipped with a quartz window and 0.1 N NaOH solution saturated with oxygen as shown in **Figure 1**. The counterelectrode was a Pt foil and a standard calomel electrode was used as reference. The working electrode was illuminated by white light from a high pressure 300W Xe lamp. Monochromatic light was obtained by interference filter. The light intensity was measured with a Eppley Thermopile, E6. A potentiostat and function generator were used for regulating the potential of working electrode. All the measurements were performed at room temperature.

### 3. Results and Discussion

#### 3.1 Effects of plasma spray condition on photoanodic properties of plasma sprayed $\text{TiO}_2$ coatings

**Figure 2** presents the current-potential curves obtained for  $\text{TiO}_2$  coatings using METCO- $\text{TiO}_2$  powder under illumination and in dark. These were typical curves for plasma sprayed  $\text{TiO}_2$  coatings electrodes. The plasma spray atmosphere were air, and Ar 100 l/min and Ar 100 l/min+hydrogen 10 l/min as plasma gas. The potential scanning rate in this study was always 400 mV/min.

Regardless of using hydrogen as plasma gas, the current of  $\text{TiO}_2$  coatings were greater under illumination than in dark, because of formation of electron-hole pair by light. And, regardless of illumination,

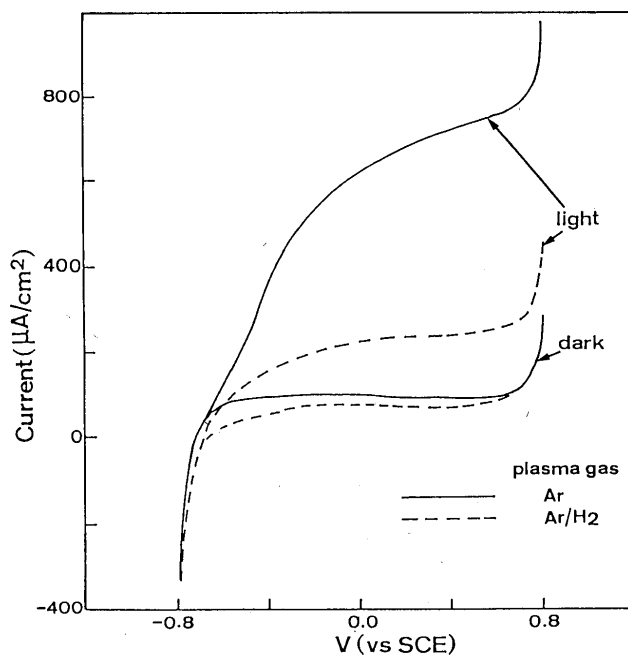


**Fig. 2** Current-potential curves for plasma sprayed  $\text{TiO}_2$  coatings produced by plasma gas Ar and  $\text{Ar}/\text{H}_2$  in air.

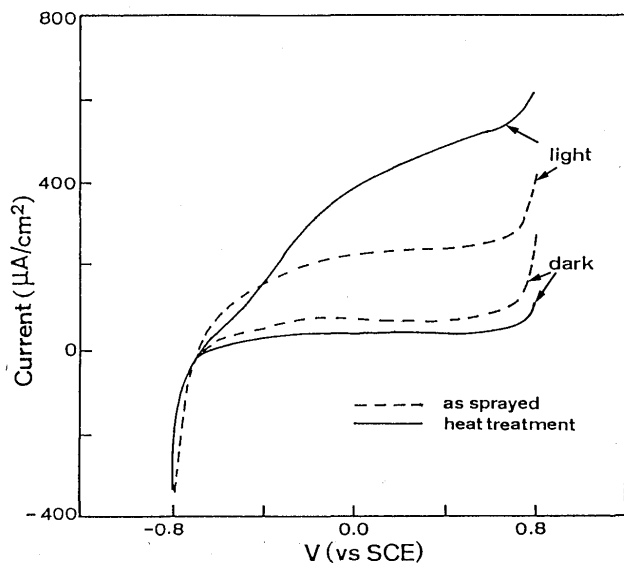


Fig. 3 Current-potential curves for plasma sprayed TiO<sub>2</sub> coatings produced by plasma gas Ar/H<sub>2</sub> in air and heat-treated at 400°C during 90 minutes.

the current and  $|E_o|$  (the absolute value of potential at zero current) of TiO<sub>2</sub> coatings produced with Ar 100 l/min were greater than with Ar 100 l/min + hydrogen 10 l/min as plasma gas.

The current of TiO<sub>2</sub> coatings produced with Ar 100 l/min as plasma gas increased greatly with increase of applied potential, and regardless of illumination,  $E_o$  (the potential value at zero current) of TiO<sub>2</sub> coatings were same value.

Figure 3 presents the current-potential curves for TiO<sub>2</sub> coatings plasma sprayed using METCO-TiO<sub>2</sub> powder and heat treated at 400°C during 90 minutes, under illumination (Xe lamp light) and in dark. The plasma spray atmosphere were air and Ar 100 l/min + hydrogen 10 l/min as plasma gas. The current of this TiO<sub>2</sub> coating increased by heat treatment. But, the current of TiO<sub>2</sub> coating heat-treated at 700°C became zero.

### 3.2 Effects of additives on photoanodic properties of plasma sprayed TiO<sub>2</sub> coatings

Figure 4 shows the current-potential curves for TiO<sub>2</sub> coatings using two kinds of powders TiO<sub>2</sub> powders (METCO) and 1wt% Y<sub>2</sub>O<sub>3</sub>-TiO<sub>2</sub> (METCO) powders. The plasma atmosphere were air and Ar 100 l/min + hydrogen 10 l/min as plasma gas and these coatings were heated in air at 400°C during 90 minutes after plasma spraying. The Xe lamp light was illuminated on the electrodes. The photocurrent for 1wt% Y<sub>2</sub>O<sub>3</sub>-TiO<sub>2</sub> coatings was greater than that of TiO<sub>2</sub> coatings and  $|E_o|$  of 1wt% Y<sub>2</sub>O<sub>3</sub>-TiO<sub>2</sub> coatings was larger than that of TiO<sub>2</sub> coatings.

Since addition of 1% Y<sub>2</sub>O<sub>3</sub> to TiO<sub>2</sub> coatings and heat treatment (400°C, 90 min.) decrease amounts of oxygen

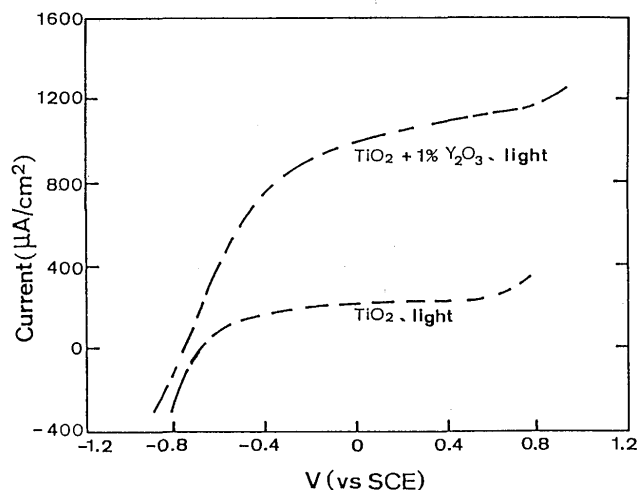


Fig. 4 Current-potential curves for plasma sprayed TiO<sub>2</sub> and 1% Y<sub>2</sub>O<sub>3</sub>-TiO<sub>2</sub> coatings produced by plasma gas Ar/H<sub>2</sub> in air and heat-treated at 400°C during 90 minutes.

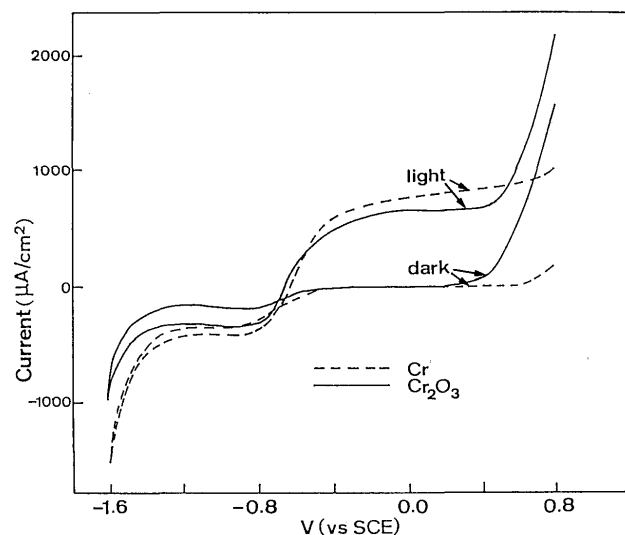


Fig. 5 Current-potential curves for plasma sprayed 1% Cr<sub>2</sub>O<sub>3</sub> and 0.5% Cr-TiO<sub>2</sub> coatings produced by plasma gas Ar in air.

loss in TiO<sub>2</sub> coatings, the photocurrent of the coating becomes higher.

Figure 5 presents the current-potential curves for TiO<sub>2</sub> coatings using two kinds of powders added 1wt% Cr<sub>2</sub>O<sub>3</sub> or 0.5wt% Cr to TiO<sub>2</sub> powders (METCO) under illumination and in dark. The plasma atmosphere was air and Ar 100 l/min as plasma gas. The anomalous photoresponse of the current-potential curves at cathodic potential were obtained by these additive to TiO<sub>2</sub> coatings comparing with the TiO<sub>2</sub> coating. Moreover, the shape of the curves depends on the wavelength of the incident light as well as on additive to TiO<sub>2</sub> coatings.

Electrons from the conduction band or from high energy surface states (lying less than 0.5 eV below the conduction band edge) contribute to oxygen reduction in the dark<sup>9,10</sup>. Oxygen reduction and the anomalous

photoresponse both occur at a potential close to  $V_{FB}$ . This behavior seems likely to us that the anomalous photoresponse could come from an enhancement of the oxygen reduction rate due to the reduction of additives.

### 3.3 Anodic current-potential and time behavior

While BG photoresponse in  $n$ -TiO<sub>2</sub> is known to be due to O<sup>-2</sup>-Ti<sup>+4</sup> electronic transitions, photogenerated holes reaching the interface with the electrolyte at the O<sub>2P</sub> band, SBG photoresponse mechanisms are not well known. The bulk band gap are involved in the sub-bandgap excitation process, can be associated with cationic impurities and/or lattice defects<sup>11</sup>.

Photocurrent, (Pc)-time relation at a fixed potential induced by intermittent illumination was examined. A typical photoresponse of  $n$ -TiO<sub>2</sub> was schematized in Figure 6. The stationary photocurrent (Pc-st) reached after enough time of illumination, and the initial photocurrent spike (Pc-in) is obtained at the moment the light illuminate by constant illumination flux (I<sub>0</sub>). When the light is turned off, the cathodic current spike (Pan-in) of back reaction is superimposed on the anodic photocurrent. This back reaction can be considered as decrease in surface potential due to illumination, photopotential and surface electron-hole recombination process<sup>12,13,14</sup>.

Figure 7 shows the ratio of Pc-st/Pc-in obtained from photocurrent-time transient behavior of TiO<sub>2</sub> coatings added 1wt% Y<sub>2</sub>O<sub>3</sub> as a function of the applied potential for BG light (380 nm), SBG light (476 nm) and Xe lamp light.

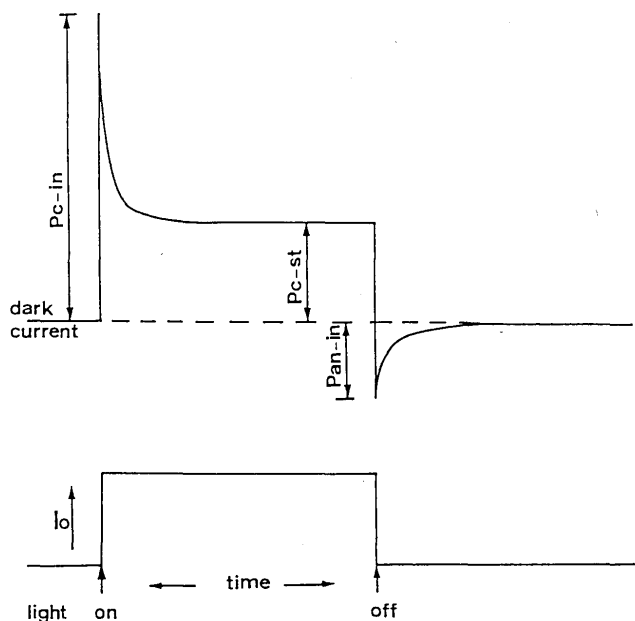


Fig. 6 Typical transient photoresponse of plasma sprayed TiO<sub>2</sub> coatings.

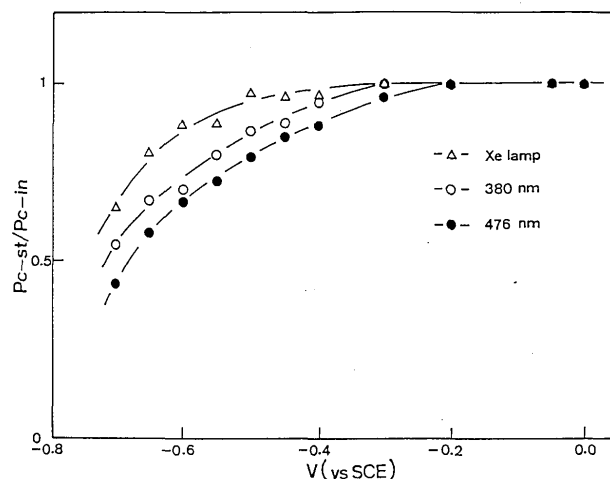


Fig. 7 Potential dependence of the transient ratio, (Pc-st/Pc-in) for photoresponse obtained with the polychromatic light of 300 W Xe lamp, 380 nm and 476 nm in 1% Y<sub>2</sub>O<sub>3</sub>-TiO<sub>2</sub> coatings produced by plasma gas Ar/H<sub>2</sub> in air and heat-treated at 400°C during 90 minutes.

From Fig. 7, at higher anodic potentials than -0.2 V, the transient practically disappears, and Pc-st/Pc-in becomes 1, which means that for every photon absorbed efficiently in the SC depletion layer a photogenerated hole is able to reach easily the interface between TiO<sub>2</sub> coatings and the electrolyte, and oxidize a water molecule<sup>11</sup>.

At cathodic potentials, the ratio decrease and is large in order of Xe lamp light, BG light (380 nm), SBG light (476 nm). Where, the light intensity is large in order of Xe lamp light, BG light (380 nm), SBG light (476 nm), and  $|E_0|$  is small in order of SBG light (476 nm), BG light (380 nm), Xe lamp light in 1% Y<sub>2</sub>O<sub>3</sub>-TiO<sub>2</sub> coatings (thickness: 40~50  $\mu$ m).

Because the Helmholtz layer is sufficiently thin, for semiconductor electrodes in the photoelectrolysis of water, the tunneling constant becomes smaller than surface recombination time constant. When the semiconductor and electrolyte are separated by a thin insulating film on semiconductor, a large value of tunneling constant should be obtained for tunneling through the film as well as the Helmholtz layer. Clearly, the thicker the film, the larger the value of tunneling constant. On the other hand, the surface recombination time constant decrease with the increase in the surface concentration of holes which can be proportional to the light intensity of illumination. Thus, for some large value of tunneling constant, it would be possible that as the intensity of illumination increases, the transition occurs from the recombination-controlled process in which the photocurrent of holes across the interface is proportional to the light intensity, to the tunneling-controlled process in which it depends little on the light intensity<sup>15</sup>.

Accordingly, we can reckon that the recombination control of transient behavior increased (i.e. the ratio,  $P_{c-st}/P_{c-in}$ , decreased) with the decrease of light intensity and  $|E_o|$  for illumination light in 1% Y<sub>2</sub>O<sub>3</sub>-TiO<sub>2</sub> coatings.

### 3.4 Photocurrent-time behavior in open circuit

The current-time behaviors of TiO<sub>2</sub> coatings in open circuit for constant illumination flux were same features, as shown in Fig. 6. In this section, abnormal photoresponse behavior was discussed.

Figure 8 shows photocurrent-time relation of TiO<sub>2</sub> coating using TiO<sub>2</sub> powders (Nihon Abrasion Ltd) contained a large amounts of Fe, for various monochromatic lights. The plasma sprayed atmosphere was air and Ar 100 l/min as plasma gas)

For 325~398 nm wavelengths, the photocurrent increased slowly to a value after much rapid increase when a light is illuminated, and decrease with time. At 476 nm wavelength, however, the photocurrent had maintained a constant value after rapid increase and decrease with time. When light was switched off, the situation was just the reverse of that when illumination started.

This kinetic response of photocurrent is a result of impurity trapping. During the initial part of the excitation, impurity holes are trapped, and later an appreciable free carrier density can be supported and photocurrent again increases. After illumination is turned off, slow decay attributed to the existence of traps within the space charge layer.

This abnormal photoresponse behavior was observed also in TiO<sub>2</sub> coatings plasma-sprayed using TiO<sub>2</sub> powders added Cr<sub>2</sub>O<sub>3</sub> or Ni. The bulk states of TiO<sub>2</sub>

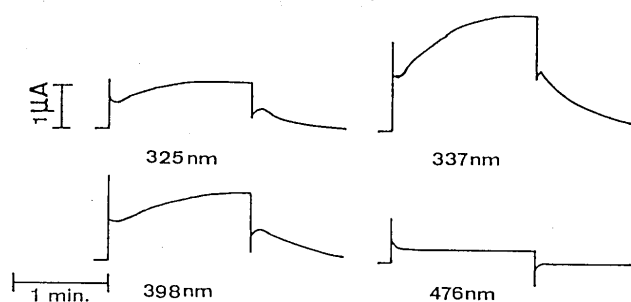


Fig. 8 Time dependence of the photocurrent and decays for various light wavelength in plasma sprayed TiO<sub>2</sub> coatings produced by TiO<sub>2</sub> powders (Nihon Abrasin Ltd).

coatings are associated with impurity (Fe, Cr and Ni ion)<sup>16,17</sup>, they revealed a band of states centered at 2.0 eV below the conduction band edge that appears to be the band surface active states in oxygen evolution.

### 4. Conclusions

- 1) The photocurrent of plasma sprayed 1wt% Y<sub>2</sub>O<sub>3</sub>-TiO<sub>2</sub> coatings was greater than that of TiO<sub>2</sub> coatings and  $|E_o|$  (potential value at zero current) of 1wt% Y<sub>2</sub>O<sub>3</sub>-TiO<sub>2</sub> coatings was larger than that of TiO<sub>2</sub> coating.
- 2) The anomalous photoresponse of the current-potential curves at cathodic potential were obtained by additive (Cr<sub>2</sub>O<sub>3</sub> or Cr) to TiO<sub>2</sub> coatings comparing with the TiO<sub>2</sub> coatings.
- 3) The kinetic responses of photocurrent were observed in TiO<sub>2</sub> coatings added Cr<sub>2</sub>O<sub>3</sub> or Ni. The bulk states of TiO<sub>2</sub> coatings are associated with impurity ion. The phenomenon is a result of the impurity trapping. During the initial part of the excitation, impurity are trapped, and later an appreciable free carrier density can be supported and photocurrent again increases.

### References

- 1) A. Fuzishima and K. Honda: Nature (Lond.), 238 (1972) pp. 37.
- 2) H. Morisaki M. Hariya and K. Yazawa: J. Appl. Phys. Lett., 30 (1977) pp. 7.
- 3) S.-E. Lindquist and A. Lindgren: J. Electrochem. Soc., 132 (1985) pp. 623.
- 4) M.R. Kozlowski, P.S. Tyler and W.H. Smyrl: Electrochem. Soc., 136 (1989) pp. 442.
- 5) S.-E. Lindquist B. Finnström and A. Lindgren: Electrochem. Soc., 130 (1983) pp. 1795.
- 6) M.F. Weber, L.C. Schumacker and M.J. Dignam: J. Electrochem. Soc., 129 (1982) pp. 2022.
- 7) P. Salvador: J. Electrochem. Soc., 128 (1981) pp. 1895.
- 8) L. Parent, J.P. Dodelet, G.G. Ross and B. Terreault: J. Electrochem. Soc., 132 (1985) pp. 2590.
- 9) F. Decker, J.F. Julião and M. Abramovich: J. Appl. Phys. Lett., 35 (1979) pp. 397.
- 10) D. Laser, M. Yaniv and S. Gottesfeld: J. Electrochem. Soc., 125 (1978) pp. 358.
- 11) P. Salvador: Surface Sci., 192 (1987) pp. 36.
- 12) R.H. Wilson: J. Electrochem. Soc., 127 (1980) pp. 228.
- 13) P. Salvador: J. Appl. Phys., 55 (1984) pp. 2977.
- 14) D. Laser and A.J. Bard: J. Electrochem. Soc., 123 (1976) pp. 1833.
- 15) M. Nishida: J. Appl. Phys., 51 (1980) pp. 1669.
- 16) Amal K. Ghosh, R.B. Lauer and R.R. Addiss, Jr.: Phys. Rev., B-8 (1973) pp. 4842.
- 17) K. Mizushima, M. Tanaka, A. Asai, S. Iida and J.B. Goodenough: J. Phys. Chem. Solids, 40 (1979) pp. 1129.